

Trace Residue Identification, Characterization and Longitudinal Monitoring of the Novel Synthetic Opioid β -U10, from Discarded Drug Paraphernalia

Henry West¹, John L. Fitzgerald², Katherine L. Hopkins^{1,2}, Michael G. Leeming³, Matthew DiRago^{4,5}, Dimitri Gerostamoulos^{4,5}, Nicolas Clark^{6,7}, Paul Dietze^{8,9}, Jonathan M. White¹, James Ziogas¹⁰ and Gavin E. Reid^{1,10,11*}

¹School of Chemistry, The University of Melbourne, Parkville, 3010, Australia

²School of Social and Political Science, The University of Melbourne, Parkville, Victoria 3010, Australia

³Melbourne Mass Spectrometry and Proteomics Facility, Bio21 Molecular Science and Biotechnology Institute, The University of Melbourne, Parkville, Victoria 3010, Australia

⁴Victorian Institute of Forensic Medicine, Southbank, Victoria, 3006, Australia

⁵Department of Forensic Medicine, Monash University, Clayton, Victoria, 3800, Australia.

⁶North Richmond Community Health, Richmond, Victoria, 3121, Australia.

⁷Royal Melbourne Hospital, Parkville, Victoria, 3050, Australia.

⁸National Drug Research Institute and enAble Institute, Curtin University, Melbourne, Victoria 3004, Australia.

⁹Disease Elimination Program, Burnet Institute, Melbourne Victoria 3004, Australia

¹⁰Department of Biochemistry and Pharmacology, The University of Melbourne, Parkville, Victoria 3010, Australia

¹¹Bio21 Molecular Science and Biotechnology Institute, The University of Melbourne, Parkville, Victoria 3010, Australia

* Corresponding author: Email: gavin.reid@unimelb.edu.au

Abstract

Empirical data regarding dynamic alterations in illicit drug supply markets in response to the COVID-19 pandemic, including the potential for introduction of novel drug substances and/or increased poly-drug combinations at the ‘street’ level (i.e., directly proximal to the point of consumption), is currently lacking. Here, a high-throughput strategy employing ambient ionization-mass spectrometry is described for the trace residue identification, characterization and longitudinal monitoring of illicit drug substances found within >6,600 discarded drug paraphernalia (DDP) samples collected during a pilot study of an early warning system for illicit drug use in Melbourne, Australia from August 2020-February 2021, while significant COVID-19 lockdown conditions were imposed. The utility of this approach is demonstrated for the *de novo* identification and structural characterization of β -U10, a previously unreported naphthamide analogue within the ‘U-series’ of synthetic opioid drugs, including differentiation from its α -U10 isomer without need for sample preparation or chromatographic separation prior to analysis. Notably, β -U10 was observed with 23 other drug substances, most commonly in temporally distinct clusters with heroin, etizolam and diphenhydramine, and in a total of 182 different poly-drug combinations. Finally, longitudinal monitoring of the number and weekly ‘average signal intensity’ (ASI) values of identified substances, developed here as a semi-quantitative proxy indicator of changes in availability, relative purity and compositions of street level drug samples, revealed that increases in the number of identifications and ASI for β -U10 and etizolam coincided with a 50% decrease in the number of positive detections and an order of magnitude decrease in the ASI for heroin.

Keywords: novel synthetic opioid, β -U10, trace residue analysis, DART, mass spectrometry

1 Introduction

To date, studies to examine changes to the illicit drug market during the current COVID-19 pandemic have largely been focused on monitoring population level trends associated with known drug substances via wastewater analysis [1-3], by conducting surveys of people who use drugs [4], and inferences from secondary indicators of drug related harms [5]. Therefore, empirical data regarding the potential for dynamic alterations in drug availability or purity, increased adulteration or poly-drug use, or the introduction of novel drug substances at the ‘street’ level (i.e., directly proximal to the point of consumption) is currently lacking. The potential for introduction of new psychoactive substances (NPS) or adulterants into the illicit drug market, including novel synthetic opioids (NSO’s), is of particular concern due to their often poorly understood pharmacological properties and potential for higher potencies compared with traditional opioid drugs (e.g., heroin, oxycodone, etc.) [6-9]. For example, in addition to the well-known fentanyl and fentanyl-analog phenylpiperidine opioid drugs, a lesser-known class of NSO’s include the ‘AH-‘ (e.g., AH-7921), and ‘U-’ series of benzamide (e.g., U-47700) and acetamide (e.g., U-50488) drugs. U-47700 is a potent μ -opioid receptor agonist, reported to be 7.5 times more potent than morphine (in animal models), while U-50488 is a κ -opioid receptor agonist [6]. Originating from the Allen and Hanburys [10,11] and Upjohn Companies [12] in the 1970’s, the AH- and U-series of drugs have never been brought to market for therapeutic use, but have increasingly appeared in the illicit drug market since the early 2010’s, with numerous fatalities reported worldwide [6,8,13-16].

Predominately, newly emerging NSO’s are identified and characterized from intact samples seized by law enforcement agencies [17], obtained during online monitoring of drug markets [18], or provided by individuals presenting for medical care after experiencing adverse effects following consumption [19], using a range of analytical chemistry techniques including Fourier-transform infrared spectroscopy (FT-IR), gas chromatography-mass spectrometry (GC-MS), liquid chromatography (LC-MS) using electrospray ionization (ESI), LC-tandem mass spectrometry (MS/MS) and Nuclear magnetic resonance (NMR). The sensitivity of GC-MS and LC-MS and -MS/MS methods also facilitate the use of these techniques for trace residue analysis of the contents of discarded drug paraphernalia (DDP), such as used syringes, where materials may be present in only microgram to nanogram quantities [20-25]. These later efforts can provide

information on the prevalence of specific drug substances, adulterants and poly-drug combinations that are in use within a specific population at the end of the supply chain and proximal to the site of consumption. However, as these methods typically use ‘targeted’ approaches for detection, and also require relatively long time frames for sample preparation and analysis that limits the scale at which they can be applied (e.g., for large-scale monitoring applications), the emergence of newly emerging NSO drugs that initially are not in widespread use within a given community may potentially go undetected [26,27].

As an alternative, a range of MS-based ‘ambient’ ionization techniques that require minimal sample preparation and with capability for higher throughput compared to GC- and LC-MS have recently been developed and applied to the trace residue analysis of illicit drug substances, including those present in biofluids (saliva, urine, blood etc.) and DDP. Examples include Desorption ElectroSpray Ionization (DESI) [28-30], Paper-Spray (PS) [31-33], Low Temperature Plasma (LTP) ionization [34], Atmospheric Solids Analysis Probe (ASAP) [35] and Direct Analysis in Real Time (DART) [36-40]. When coupled with high-resolution accurate mass spectrometry and MS/MS techniques, the identification and characterization of unexpected or novel drug substances may potentially be achieved using these approaches, via assignment of the molecular formulae of the observed ions and by similarities in MS/MS fragmentation behavior compared to structurally homologous known substances within an established drug class [41-44].

Recently, we described the development and application of a DART-MS and -MS/MS approach for rapid and high-throughput trace residue sampling and analysis of discarded drug packaging samples (DPS) as part of an early warning monitoring system for illicit drug use at large public events. This approach was shown to be applicable for the identification and characterization of a wide range of illicit drugs and adulterant substances, including numerous NPS and complex poly-drug mixtures, using laboratory-based instrumentation as well as in ‘close-to-real-time’ applications using a transportable mass spectrometer housed within a mobile analytical laboratory [40]. Here, we describe the extension of this approach for the identification of substances present within >6,600 DDP samples collected during a six-month pilot study between September 2020 and February 2021 in Melbourne Australia while significant COVID-19 lockdown conditions were in place. Notably, this enabled the *de novo* identification and structural characterization of a previously unreported naphthamide analogue within the ‘U-series’ of NSO drugs, namely β -U10, that was observed in over 800 samples and in temporally distinct clusters throughout the study.

Furthermore, we also report the development of a semi-quantitative strategy for longitudinal monitoring of the number and weekly average signal intensity (ASI) of identified substances, including β -U10, as a proxy for changes in the availability, relative purity and compositions of ‘street level’ drug samples.

2. Materials and Methods

2.1 Chemicals and Reagents

1-naphthyl chloride, 2-naphthyl chloride, LC-MS grade dichloromethane, LC-MS grade ethyl acetate, methanol, sodium sulfate, sodium hydroxide and triethylamine were purchased from Sigma Aldrich (Castle Hill, NSW, Australia). (1*R*,2*R*)-*N,N,N'*-trimethyl-1,2 diaminocyclohexane was purchased from BLD Pharmtech Ltd (Shanghai, China). Cotton tip applicators were purchased from Swisspers (Kingsgrove, NSW).

2.2 DDP sample collection and preparation

DDP consisting of used 1 mL, 3 mL and other volume syringes, plastic spoons, aluminium trays, and DPS including disposable plastic ziplock bags, aluminium foil, plastic wrap, and other items, were collected once-weekly (estimated number of 500 – 1000 items total per week) from established service providers across metropolitan Melbourne, Victoria Australia, during a 24-week pilot study from August 2020 to February 2021 (20 weeks from August 3rd, 2020 to December 11th, 2020 and another 4 weeks from January 11th, 2021 to February 5th, 2021). This period of time coincided with a strict lockdown imposed across metropolitan Melbourne from August 2nd, 2020 to October 18th, 2020 due to the COVID pandemic, which included a two-hour daily time limit for outdoor activities, a 5 km (3.1 mile) radius restriction on outdoor movement from the primary residence, and a night time curfew from 8 p.m. to 5 a.m. This was followed by a series of stepwise relaxation of restrictions until November 8th, 2020, after which travel was allowed to and from anywhere in the state. From approximately 500-1000 DDP collected each week, an average of 276 per week were selected for analysis (6,631 samples total, Table 1).

Table 1. Summary of the number and type of DDP samples analyzed during this study.

Syringe (1 mL)	Syringe (3 mL)	Syringe (other vol.)	Plastic Spoon	Metal Tray	DPS ¹	Other ²	Total
4738	781	21	341	221	494	35	6631

71.5%	11.8%	0.3%	5.1%	3.3%	7.5%	0.5%	
-------	-------	------	------	------	------	------	--

¹DPS as defined in [40].

²Samples categorised as “other” included glass ‘pipes’, glass ampules and teaspoons.

A syringe decapitator was used to safely remove the needle from syringes, followed by plunger removal and visual inspection. Samples were then prepared for analysis by lightly swabbing the surface area of the DDP (e.g., the inside of the barrel of syringes, the inner surface of plastic spoons or metal trays, or the interior of ziplock bags as previously described [41]) using commercially available cotton tip applicators (Swisspers, Kingsgrove, NSW, Australia). The majority of DDP samples contained no visible residue. However, for samples containing visible residue, the cotton tip applicators were gently flicked after swabbing to displace any loose material. Samples containing blood, saline or other liquids were swabbed and then allowed to dry prior to analysis.

2.3 Direct Analysis in Real Time – Mass Spectrometry (DART-MS) and tandem mass spectrometry (MS/MS) of DDP samples

Samples were introduced to a Thermo Scientific Q Exactive Plus (Bremen, Germany) mass spectrometer using a Direct Analysis in Real Time (DART) source and a Vapor Interface (IonSense, MA, USA), as previously described [40]. The probe heater was set to 200°C using nitrogen as the ionizing gas. Swabs were positioned between the probe and the Vapor interface using a probe position setting of 6 (arbitrary value). The transfer capillary temperature of the mass spectrometer was set to 250°C. Ultra High Resolution / Accurate Mass Spectra (UHRAMS) were acquired over a range of m/z 100 – 500 in positive ionization mode. HCD-MS/MS spectra were acquired using an isolation window of +/- 0.5 or 1 m/z , with a normalized collision energy set between 10 and 40% depending on the precursor ion of interest. For both MS and MS/MS experiments, ions were detected using the Orbitrap mass analyser operating with a mass resolving power of 17,500 (at 200 m/z) and an AGC target of 1.0E6. Spectra were averaged across 100 scans with MS data collected in 6 seconds and HCD-MS/MS in 10 seconds. Blank cotton swabs were run every 5 samples as controls.

2.4 Data analysis, identification and semi-quantitative ‘average signal intensity’ (ASI) calculations

A database of illicit drug substances, known adulterants, bulking agents and common contaminants was compiled (over 1000 substances in total at the time of writing, and regularly updated as new substances are reported in both the literature and publicly-available databases including NPS discovery [45]), along with the exact m/z values for their $[M+H]^+$ ions. Thermo ‘.raw’ files produced by DART-MS analysis were first converted to ‘.mzML’ format using msconvert [46] (v3.0.21040.fbf7857be) with vendor-specific peak centroiding activated. Individual mass spectra were then accessed using a python (v3.7.5) script developed in-house, using the pymzml [47] (v2.4.7) library and the summed intensities of ions within +/- 5 ppm of the theoretical $[M+H]^+$ m/z value of each substance in the database were extracted. Given that the total ion current (TIC) of individual spectra acquired from each sample using DART often varied substantially over the acquisition period, individual spectra with the lowest 50% TIC were first excluded, then target abundances were computed by averaging the signal intensities from the remaining spectra. The python scripts used for processing are available from the authors upon request. Positive identifications were assigned only if the signal intensity for the precursor ion of interest was greater than the limit of detection (defined as the mean + 3 times the standard deviation of the blank) and greater than an arbitrary absolute threshold of $1E4$, below which high quality MS/MS spectra for more species could not be acquired for definitive identification. Calculation of weekly ASI values were achieved by averaging the processed signal intensities for the individual substances identified in each sample, from each week of analysis.

2.5 Synthesis of α -U10 reference standard

(1*R*,2*R*)-*N,N,N'*-trimethyl-1,2 diaminocyclohexane (500 mg, 3.20 mmol) and triethylamine (0.45 mL, 3.22 mmol) were added to a solution of 1-naphthoyl chloride (0.40 mL, 2.95 mmol) in dry dichloromethane (15 mL) then stirred at room temperature for 20 hours. The sample was then cooled on ice, followed by the addition of aqueous sodium hydroxide (1 M) and stirred again for one hour. The organic layer was extracted using ethyl acetate, washed with sodium hydroxide (1 M) followed by chilled water, then dried over sodium sulfate and further concentrated

under a stream of nitrogen to yield a white powder. Recrystallisation from hot ethyl acetate yielded colorless cubic crystals (40% yield).

2.6 *Synthesis of β -U10 reference standard*

(1*R*,2*R*)-N,N,N'-trimethyl-1,2 diaminocyclohexane (500 mg, 3.20 mmol) and triethylamine (0.45 mL, 3.22 mmol) were added to a solution of 2-Naphthoyl chloride (484 mg, 2.95 mmol) in dry dichloromethane (15 mL) and stirred at room temperature for 20 hours, forming an oil. Ethyl acetate was then added and sonicated for 5 minutes to give an off-white powder. The powder was recrystallized from ethyl acetate and washed with a MeOH:H₂O (50:50) solution, yielding colorless cubic crystals (20% yield).

2.7 *X-ray crystallography of the α -U10 and β -U10 reference standards*

Intensity data for the α -U10 and β -U10 reference materials were collected on a Rigaku XtaLAB Synergy at 100.0(1) K. The temperature was maintained using an Oxford Cryostream cooling device. The structures were solved by direct methods and difference Fourier synthesis [48]. Thermal ellipsoid plot were generated using the program Mercury [49] integrated within the WINGXⁱ suite of programs [50]. The N-methylamide moiety in α -U10 adopted a *trans*-configuration O(1)-C(10)-N(1)-C(7) -178.2(3)°, while the corresponding moiety in β -U10 adopted a *cis*-configuration C(11)-C(10)-N(1)-C(7) 179.48(14)° (**Figure 1**). α -U10: C₂₀H₂₆N₂O, *M* = 310.43, *T* = 100.0 K, λ = 1.54184 Å, Monoclinic, space group P2₁, *a* = 7.6316(3) *b* = 14.9235(4), *c* = 8.2482(3) Å, β = 117.062(5)° *V* = 836.54(6) Å³, *Z* = 2, *D*_c = 1.232 mg M⁻³, μ = 0.589 mm⁻¹, *F*(000) = 336, crystal size 0.36 x 0.29 x 0.16 mm³, 9533 reflections measured θ_{\max} = 77.67°, 3417 independent reflections [*R*(int) = 0.062], the final *R* was 0.0513 [*I* > 2 σ (*I*), 3317 data] and *wR*(*F*²) was 0.1400 (all data), *GOF* 1.077, absolute structure parameter -0.2(3). CCDC deposit code 2123011: β -U10: C₂₀H₂₆N₂O, *M* = 310.43, *T* = 100.0 K, λ = 1.54184 Å, Orthorhombic, space group P2₁2₁2₁, *a* = 7.6310(1) *b* = 14.0564(1), *c* = 16.5058(2) Å, *V* = 1770.48(3) Å³, *Z* = 4, *D*_c = 1.165 mg M⁻³, μ = 0.557 mm⁻¹, *F*(000) = 672, crystal size 0.56 x 0.24 x 0.23 mm³, 21105 reflections measured θ_{\max} = 77.72°, 3731 independent reflections [*R*(int) = 0.036], the final *R* was 0.0328 [*I*

> $2\sigma(I)$, 3614 data] and $wR(F^2)$ was 0.0868 (all data), GOF 1.049, absolute structure parameter - 0.09(12). CCDC deposit code 2123012.

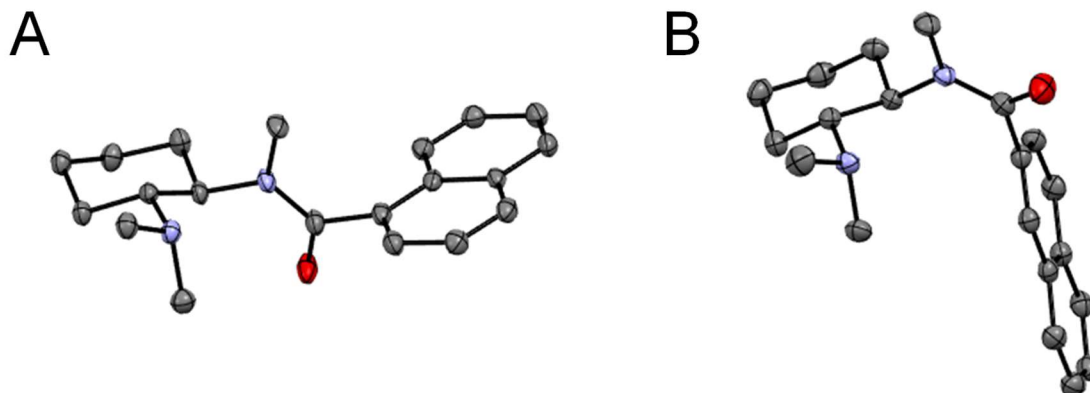


Figure 1. Thermal ellipsoid plots for the authentic reference standards of (A) α -U10 and (B) β -U10. Ellipsoids are at the 50% probability level.

2.8 *ESI-HCD-MS/MS and UVPD-MS/MS of the m/z 311.21 ion and authentic reference standards*

Selected DDP samples containing visible residue extracted into either methanol or water, and the authentic reference standards dissolved in either methanol or water, were introduced to an Orbitrap Fusion Lumos mass spectrometer (Thermo Scientific, San Jose, CA, USA) via direct infusion using a Triversa Nanomate nESI source (Advion, Ithica, NY, USA) operating with an ionization potential of 1.40 kV and gas pressure of 0.30 psi. HCD-MS/MS spectra on the m/z 311.21 precursor ions were acquired using the Orbitrap analyzer operating at a mass resolving power of 17,500 (at 200 m/z) and an AGC target of 100%, over an m/z of 50 – 350 using an isolation window of ± 0.4 m/z and with the normalized collision energy set between 10 to 50%. 213 nm UVPD-MS/MS spectra were collected using an irradiation time of 100 ms.

2.9 *Gas Chromatography – Mass Spectrometry (GC-MS) of the m/z 311 ion and authentic α -U10 and β -U10 reference standards*

GC-MS was performed using an Agilent 6890 Series GC System (Santa Clara, CA, USA) equipped with an Agilent 5973 Mass Selective Detector. Sample, dissolved in either methanol or water, were introduced to a 30 m x 0.25 mm x 0.25 μ m Zebron ZB-5MS column (Phenomenex, Torrance, CA, USA), using 1 mL/min He as the carrier gas. The injection parameters were: split ratio = 1:15; injection volume = 1 μ L (manual injection). The temperature conditions were: injector: 280°C; MSD transfer line: 280°C; MS source: 200°C; oven program: i) 90°C initial temperature for 2.0 min, ii) ramp to 300°C at 14°C /min, and iii) Hold at 300°C for 10.0 min. EI mass spectra were acquired following a solvent delay of 2 min, over an m/z range of 34-550, with a threshold of 100.

2.10 Liquid Chromatography – Mass Spectrometry (LC-MS) of the m/z 311 ion and authentic reference standards

LC-MS analysis was performed using a Shimadzu Nexera X2 HPLC coupled to a Shimadzu 8050 triple quadrupole mass spectrometer. A Phenomenex Kinetex C₁₈ column (4.6 mm x 50 mm, 2.6 μ m particle diameter) was used. The chromatographic conditions were identical to those reported by Di Rago *et. al.* [27].

2.11 Ethics and regulatory approvals

This study was approved by the University of Melbourne Human Research Ethics Committee. Approval for the collection, analysis and storage of the illicit drugs of interest was granted under the terms of a permit to purchase or otherwise obtain poisons or controlled substances for industrial, educational or research purposes granted to the Bio21 Molecular Science and Biotechnology Institute at the University of Melbourne, under the Drugs, Poisons and Controlled Substances Act 1981 (No. 9719).

3. Results and Discussion

3.1 Trace level DART-MS and -MS/MS analysis of discarded drug paraphernalia

Throughout the course of this 24-week pilot study, 6,631 DDP samples (an average of 278 per week) that were suspected to contain residual drug material were analyzed by DART-MS and -MS/MS. 5,704 (86%) tested positive for at least one catalogued drug substance. Starting the week of September 14th, 2020, a prominent but unknown ion at m/z 311.2122 (calc. composition $C_{20}H_{27}N_2O$) was observed in combinations with various known drug substances (**Figure 2**), that was not observed in the control blank samples. **Panel A in Figure 2** shows the spectrum obtained from a plastic spoon, the first sample in which this m/z 311.21 ion was observed, that also tested positive for heroin (calc. m/z 370.1655) and etizolam (calc. m/z 343.0779), a thienodiazepine drug that is not approved for medical use in Australia [51]. Other representative spectra, including from analysis of a plastic 1 mL syringe also containing etizolam and paracetamol (calc. m/z 152.0706), a metal tray also containing heroin, etizolam, cocaine (calc. m/z 304.1549), diphenhydramine (calc. m/z 256.1701), MDMA (calc. m/z 194.1181) and methamphetamine (calc. m/z 150.1283), and a metal tray also found to contain heroin, diphenhydramine, noscapine (calc. m/z 413.1547), papaverine (calc. m/z 340.1543), acetylcodeine (calc. m/z 342.1700), monoacetylmorphine (calc. m/z 328.1543) and xylitol (calc. m/z 153.0788), are shown in **Figure 2 panels B-D**, respectively. The HCD-MS/MS spectra used to definitely confirm the identity of each of these known substances are shown in **Figure 3**.

This unknown ion at m/z 311.2122, subsequently identified and characterized as β -U10 (see below), was observed a total of 838 times throughout the course of this study, most commonly in combination with (i) heroin and etizolam (130 times), (ii) heroin (81 times), (iii) diphenhydramine (74 times), (iv) heroin and diphenhydramine (44 times), (v) etizolam (27 times), and (vi) heroin, etizolam and diphenhydramine (27 times), and only 37 times on its own. However, these combinations represented only 50% of the samples in which β -U10 was observed, and overall, β -U10 was found in combination with 23 other drug substances in a total of 182 different poly-drug combinations containing up to 7 additional substances. A matrix plot showing each of the detected drugs, drug combinations, and the number of times each were observed, is shown in

Figure 4 for combinations observed at least twice, and in **Figure 5** for combinations detected only once.

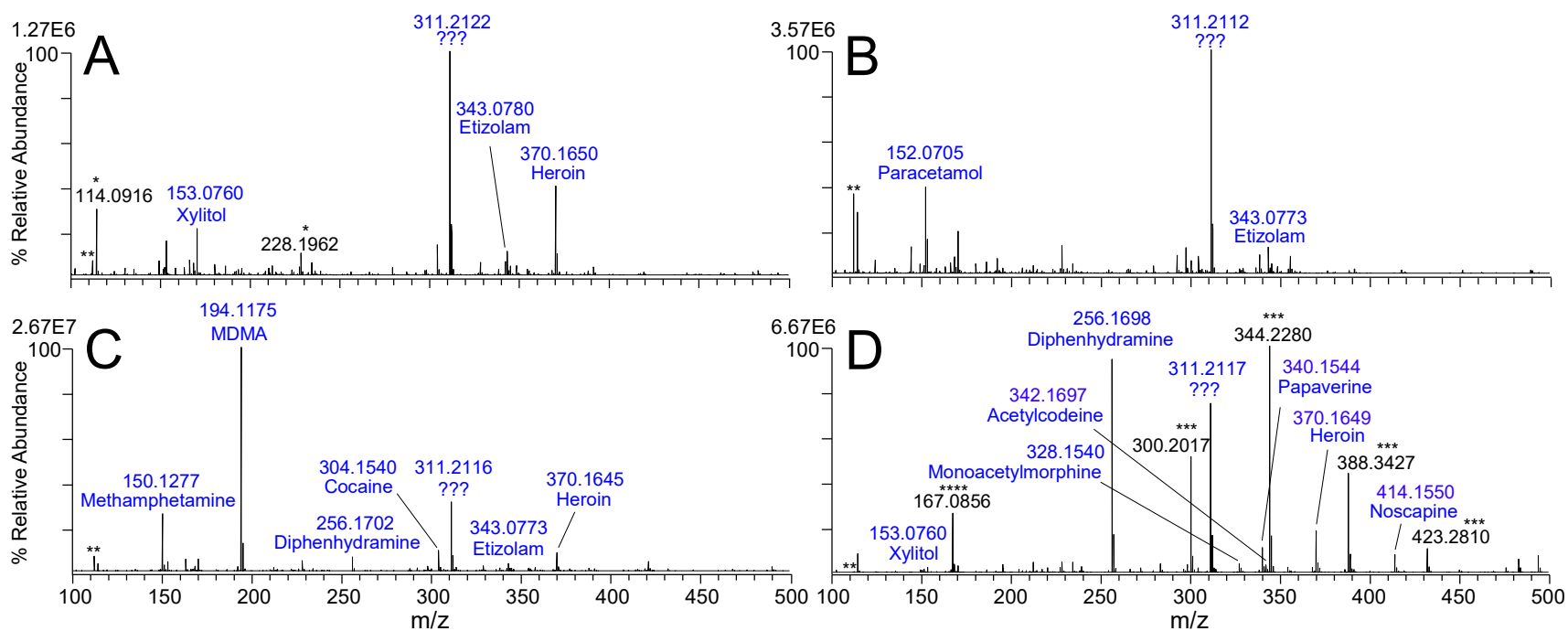


Figure 2. DART-UHRAMS trace residue analysis of DDP containing an unknown ion at m/z 311.2122 (calc. composition $C_{20}H_{27}N_2O$). Spectra resulting from analysis of (A) a plastic spoon also containing heroin and etizolam (B) a plastic 1 mL syringe also containing etizolam and paracetamol, (C) a metal tray also containing heroin, etizolam, cocaine, diphenhydramine, MDMA and methamphetamine, and (D) a metal tray also containing heroin, diphenhydramine, noscapine, papaverine, acetylcodeine, monoacetylmorphine and xylitol. * background ions. ** ammonium ion adduct of dimethylsulfone. *** PEG polymers arising from the diphenhydramine capsules. **** in-source fragment of diphenhydramine.

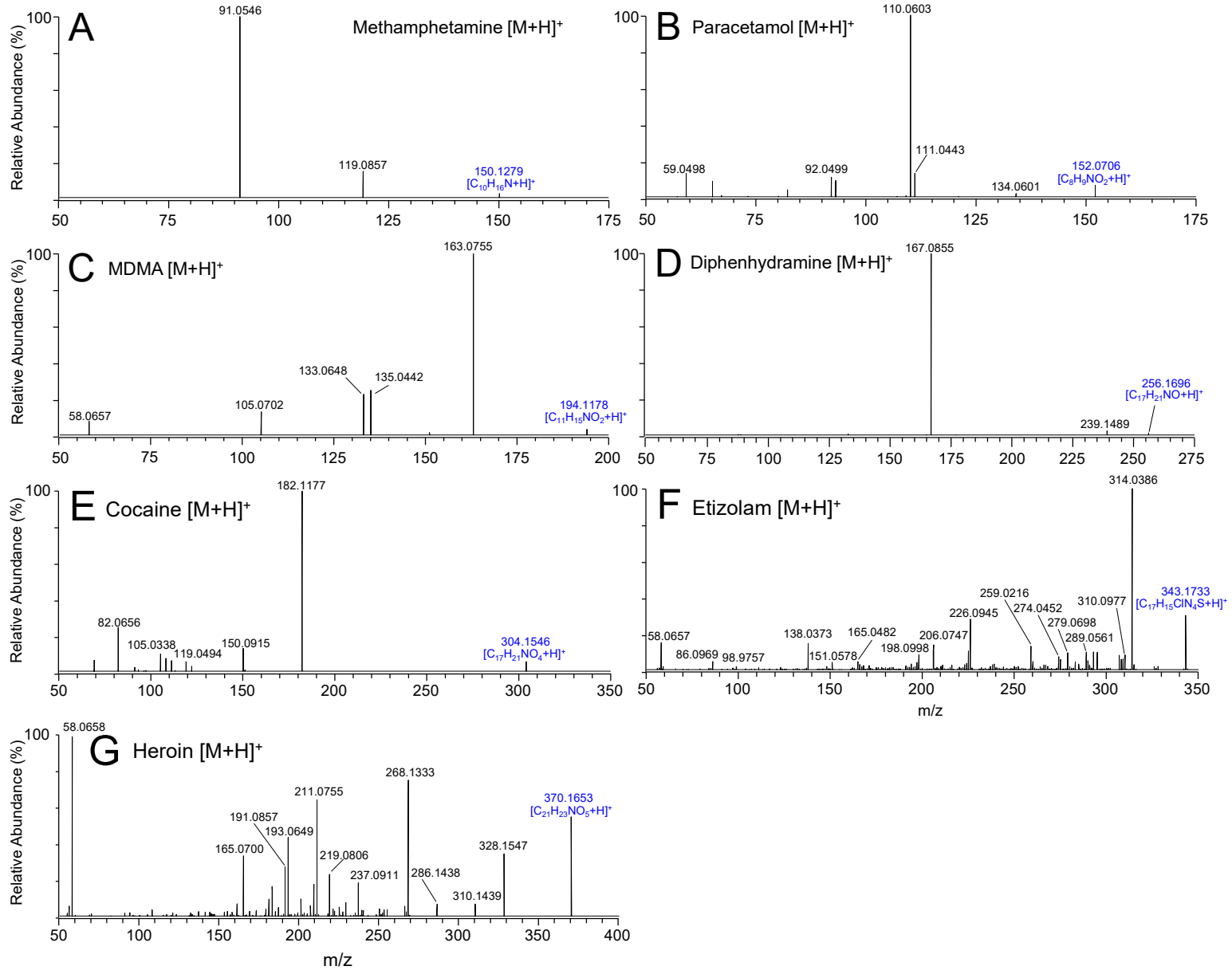


Figure 3. HCD-MS/MS of the $[M+H]^+$ precursor ions for (A) methamphetamine from Figure 2C, (B) paracetamol from Figure 2B, (C) 3,4-methylenedioxymethamphetamine (MDMA) from Figure 2C, (D) diphenhydramine from Figure 2D, (E) cocaine from Figure 2C, (F) etizolam from Figure 2B and (G) heroin from Figure 2A.

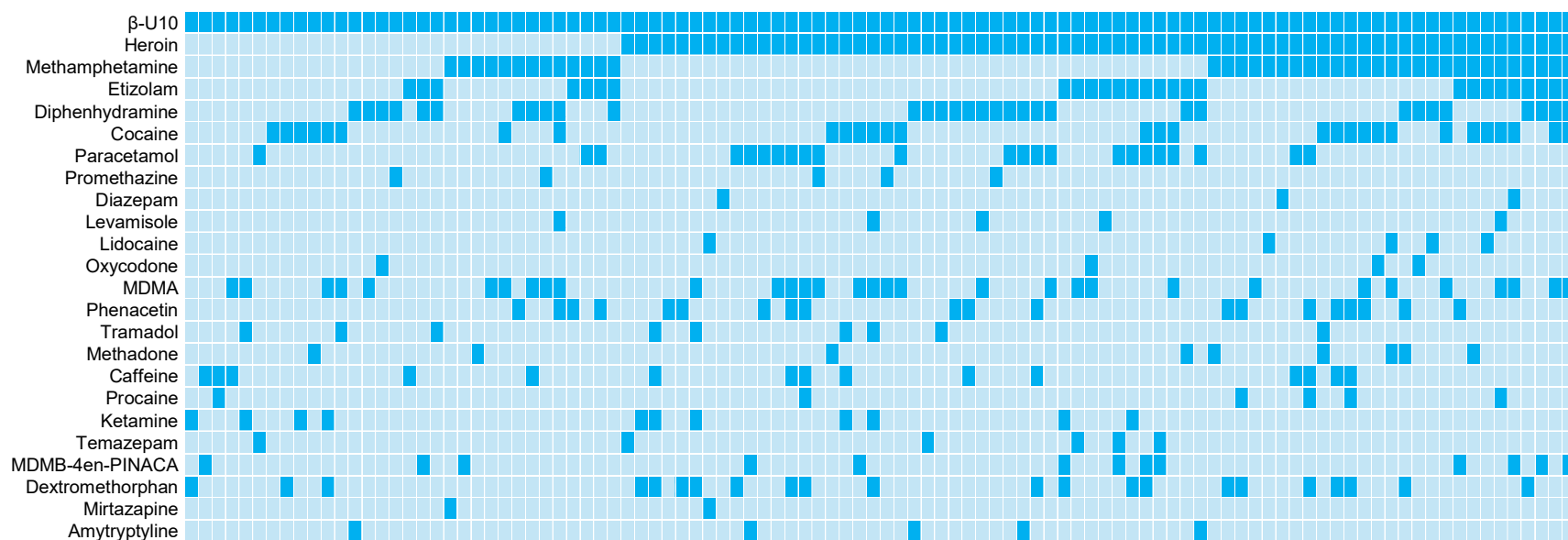


Figure 5. Summary of β -U10 drug combinations identified by trace residue DART-MS analysis, observed in at least one DDP sample.

3.2 *Longitudinal monitoring of weekly drug identifications and ASI values.*

As the majority of DDP samples containing no visible residue, this study involved trace residue analysis only. Thus, no quantitative information could be obtained regarding the absolute or relative amounts of β -U10 or other drug substances that were present. However, as a large number of samples were available to be analyzed each week, it was of interest to determine whether changes in the number of detections of a particular drug, or their relative signal intensity in the mass spectra, could potentially serve as proxy-indicators of changing market conditions, particularly those that may have occurred in response to COVID lockdown restrictions in Melbourne during the time period when the pilot study was performed. To achieve this, the individual signal intensity of drugs identified in each sample were extracted from the mass spectra then filtered using the procedure described in the Methods section above, prior to averaging the processed signal intensities of all samples in each week of analysis to generate a set of weekly ASI values. For example, plots showing the individual signal intensities and total number of detections for heroin, etizolam and β -U10 during each week of the pilot study, and their \log_{10} ASI values, are presented in **Figure 6**.

Notably, a significant decrease in the ASI for heroin was observed starting the week of October 12, before reaching a minimum in the week of November 9 at a level one order of magnitude lower than that seen in the first week of the study (**Figure 6A**). This was then followed by a gradual increase over several weeks, and stabilization, albeit not back to original levels, at the end of the study. Coinciding with this decline in ASI was a >50% decrease in the number of weekly samples that tested positive for heroin. Preceding this decline by several weeks was the onset of the appearance of both β -U10 and etizolam, whose number of detections rapidly increased over several weeks while experiencing relatively constant ASI values, and that overlapped with the decrease in number of identification and ASI for heroin. As the heroin ASI then rebounded, both the number of detections and ASI of β -U10 and etizolam decreased. In contrast, the number of weekly identifications for methamphetamine, that was observed in combination with β -U10 only 125 times throughout the study, fluctuated significantly on a weekly basis, but its ASI remained relatively constant (a difference of only 3-fold was observed over the 24-week pilot). (**Figure 7**).

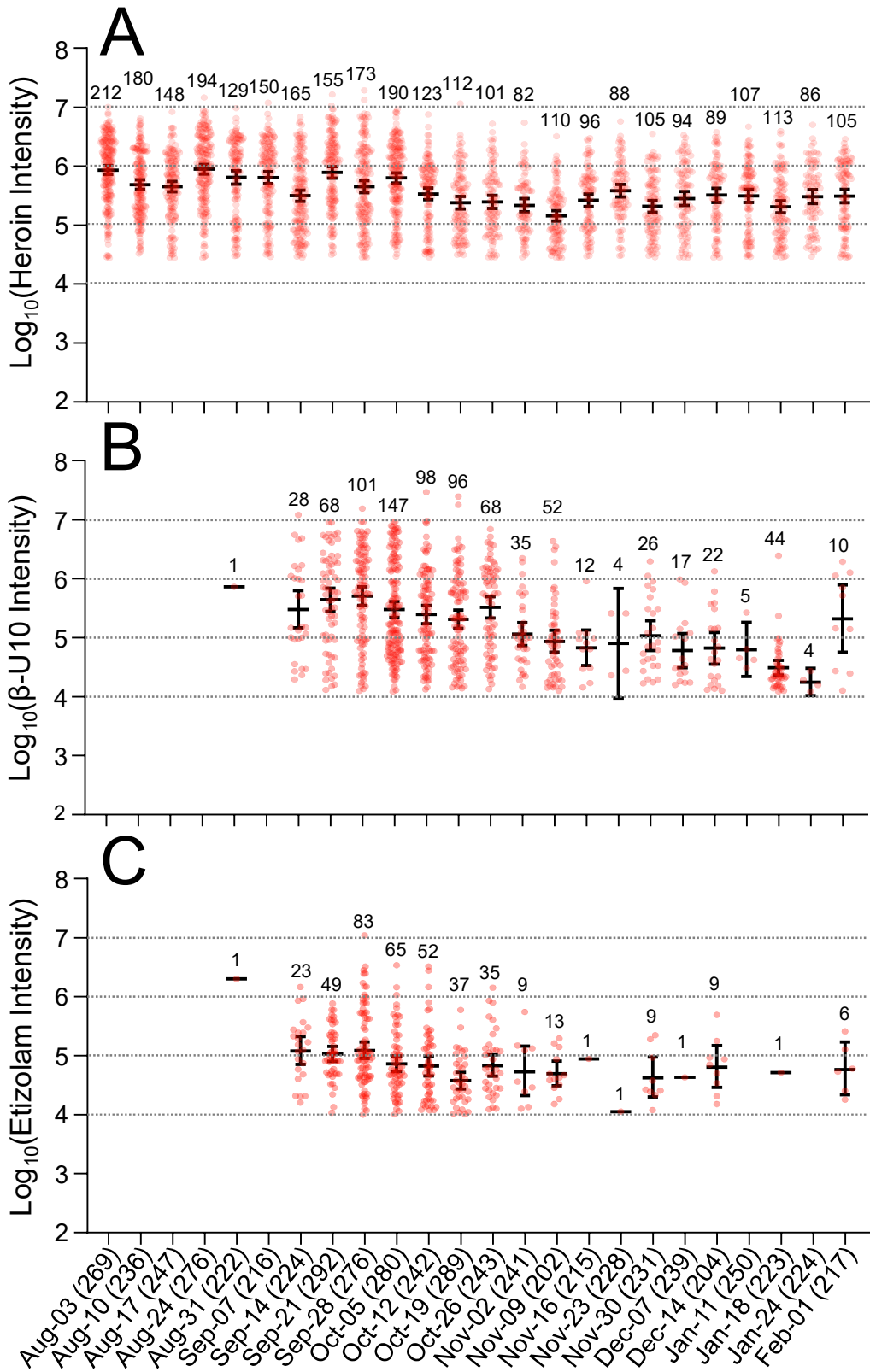


Figure 6. Weekly \log_{10} average signal intensity and number of detections for A) heroin, B) β -U10 and C) etizolam. The plot shows the average signal intensity and 95% confidence intervals each week, with individual signal intensity values shown in red and the total number of samples in which the drug was identified listed numerically. The horizontal axis label indicates the week in which the sample collection and analysis occurred, while the number in parenthesis indicates the number of samples that tested positive for at least one drug substance.

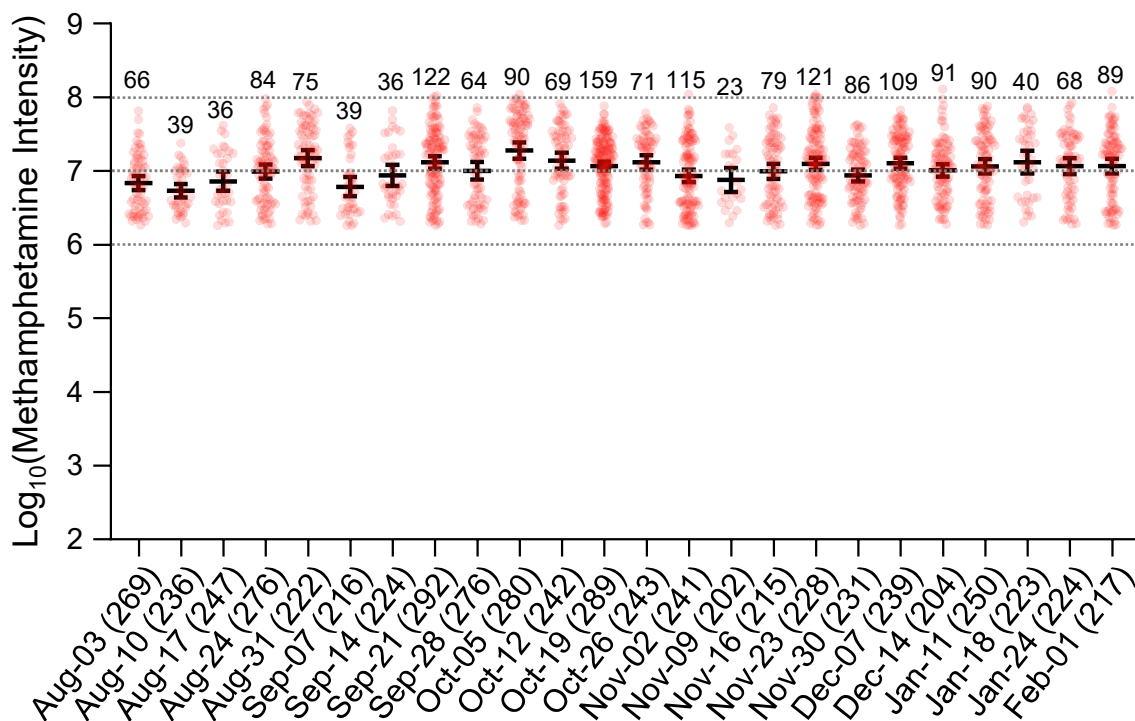


Figure 7. Weekly \log_{10} average signal intensity and number of detections for methamphetamine. The plot shows the average signal intensity and 95% confidence intervals each week, with individual signal intensity values shown in red and the total number of samples in which methamphetamine was identified listed numerically. The horizontal axis label indicates the week in which the sample collection and analysis occurred, while the number in parenthesis indicates the number of samples that tested positive for methamphetamine.

3.3 Trace level de-novo structural elucidation and characterization of the m/z 311.21 ion as U10.

UHRAMS analysis enabled a molecular formula of $C_{20}H_{25}N_2O$ to be proposed for the m/z 311.2122 ion shown in Figure 2A. HCD-MS/MS spectra of the m/z 311.2122 ion at multiple collision energies were then acquired in an attempt to assign its identity (see **Figure 8**). However, the experimentally observed fragmentation behavior did not match any available reference MS/MS spectra for substances with the proposed molecular formula. Furthermore, the spectrum was significantly different to that of any of the drug compound classes that had previously been observed in this, or our previous studies [40]. Conventional Higher energy Collision induced Dissociation (HCD)-MS/MS at low relative collision energy provided only limited structural information, with a single dominant product ion at m/z 266.15 corresponding to the loss of C_2H_7N : either dimethylamine or ethylamine (Figure 8A). Upon increasing the collision energy, however, further fragmentation of the initial m/z 266.15 product yielded significant additional structural information (Figure 8B). As a starting point, product ions were annotated with their calculated molecular formula and corresponding neutral losses relative to the ion at m/z 266.15. The base peak at m/z 155.0492, with a formula of $C_{11}H_7O^+$, was assigned as an acylium ion of naphthalene, with a corresponding ion at m/z 129.0700 resulting from the loss of CO. There is little ambiguity in these identifications as few stable ions could possess these formula. The m/z 155.0492 ion and its neutral loss of $C_7H_{13}N$, inferred the presence of an amide group, with the naphthalene group on the C=O side. Further evidence for an amide was provided by the ion at m/z 58.03, corresponding to $C_2H_4ON^+$, likely to be N-methylamide. The ion at m/z 81.07 was suspected to be a cyclohexyl moiety ($C_6H_9^+$), connected to the nitrogen of the amide, with a complimentary product ion at m/z 186.09 supporting a cleavage between the nitrogen of the amide and the cyclohexyl ring. Several candidate structures generated from this information were entered into SciFinder, where using substructure and similarity searches, a compound termed U10 (i.e., *N*-[2-(dimethylamino)cyclohexyl]-*N*-methylnaphthalene-1-carboxamide (herein termed α -U10)), was retrieved from a report by Hsu *et. al* [52]. Further searching located a monograph in the SWGDrug database [53] containing characterization data for α -U10 including GC-MS, NMR and FT-IR, but no ESI-MS/MS spectrum.

α -U10, and its *N*-[2-(dimethylamino)cyclohexyl]-*N*-methylnaphthalene-2-carboxamide (i.e., β -U10) isomer, first described by the Upjohn Company in the 1970's [12], are structural analogues of the well-known 'U-series' of synthetic *N,N*-dimethylcyclohexylbenzamide drugs, for which U-47700 has been widely reported as being responsible for, or contributing to, numerous deaths around the world [54-58]. Since 2017, when U-47700 was first subjected to regulatory controls, a range of additional structurally related compounds have appeared in the illicit drug market [59]. A comparison of the available MS/MS spectra for U-47700 [60], and other U-47700 analogues such as 3,4-methylenedioxy U-47700 [61] against the MS/MS spectrum in Figure 8 revealed fragmentation patterns that were homologous with the expected fragmentation and structures of the α -U10 or β -U10 isomers, albeit not being able to distinguish one from the other.

The U-series of *N,N*-dimethylcyclohexylbenzamide drugs have isomeric counterparts assigned as AH- (or A-), originating from the Allen and Hanburys company in the 1970's [10]. U-47700 and AH-7921 are the most well-known isomeric pair [15]. Whilst both families of drugs belong to the *N,N*-dimethylcyclohexylbenzamide class, there are key differences in their structures. U-series compounds have a 1,2-substituent arrangement on the cyclohexyl ring whilst AH-series compounds have a geminal (1,1) configuration. For U-series compounds the *N*-methylamide nitrogen is bonded directly to a carbon on the cyclohexyl ring, while AH-series compounds bridge the amide nitrogen to the cyclohexyl ring via a methylene group. These structural differences give rise to different fragmentation behaviors such that the MS/MS spectra of U-47700 and AH-7921 can be readily differentiated from each other [54,60]. For example, for U-series compounds, a product ion at 81.07 *m/z* is observed, corresponding to $C_6H_9^+$, whereas AH-series compounds show an analogous ion 14 Da higher at *m/z* 95.09, corresponding to $C_7H_{11}^+$, the cyclohexyl moiety incorporating the methylene group. Furthermore, U-series compounds give a product ion at *m/z* 58.03, corresponding to the methylamide fragment. This dissimilarity in fragmentation with AH-7921 allowed us to rule out the presence of 'A10' isomers in the sample encountered here [62].

In many of the samples where the *m/z* 311.21 β -U10 ion was observed, another ion at *m/z* 298.18 was also present, with a predicted molecular formula of $C_{19}H_{23}NO_2$ (calc. $[M+H]^+$ 298.1802). An example DART-MS spectrum obtained by trace residue sampling of a ziplock bag also containing heroin, xylitol and β -U10, along with the HCD-MS/MS spectrum of the *m/z* 298.1797 ion, is shown in **Figure 9**. Based on the predicted molecular formula, and the

fragmentation similarity with U10 seen in Figure 8, we propose this to be the protonated ester analog of β -U10, potentially formed as a by-product when synthesis of N,N,N'-trimethyl-1,2-diaminocyclohexane, a key precursor involved in β -U10 synthesis proceeded through a 2-dimethylaminocyclohexanol intermediate using the same process outlined in the patent from the Upjohn Company [12], or an analogous pathway.

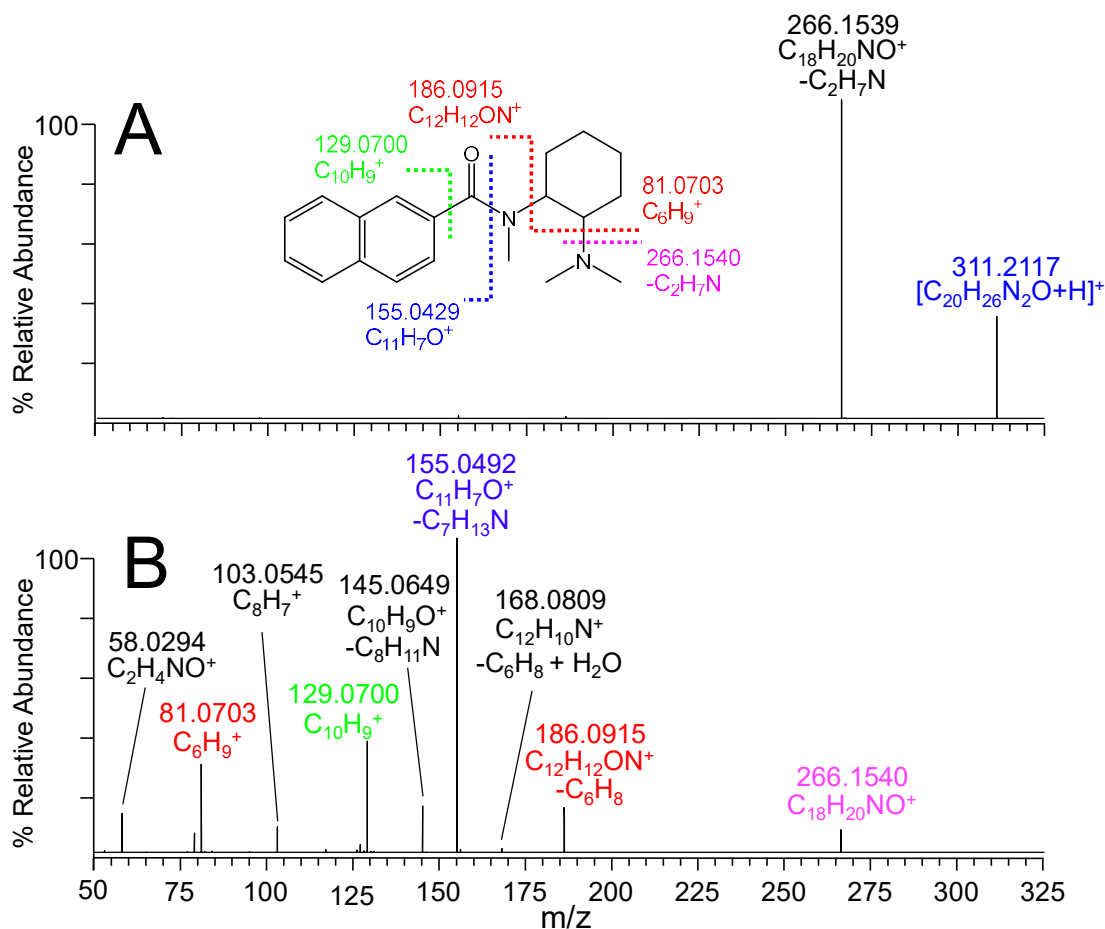


Figure 8. DART HCD-MS/MS of the m/z 311.2122 ion from Figure 2A at (A) ‘low’ 15% and (B) ‘high’ 35% normalized collision energies. Neutral losses in panel B are shown relative to the initial m/z 266.15 ion. The inset structure in panel A shows the proposed cleavage sites for β -U10.

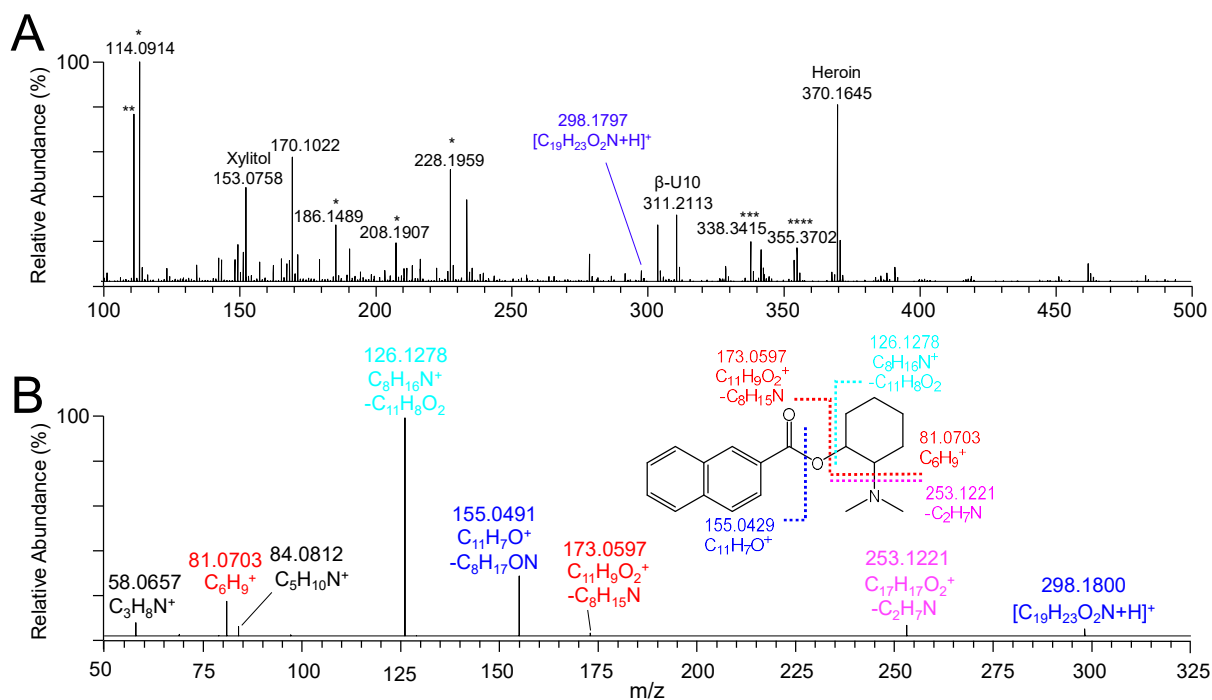


Figure 9. DART-MS and MS/MS analysis of the trace residue content of a ziplock bag containing heroin, xylitol, β -U10 and an unknown ion at m/z 298.1797, proposed to be the protonated ester analog of β -U10 ($C_{19}H_{23}NO_2$ calc. m/z 298.1802). (A) DART-MS spectrum. (B) HCD-MS/MS of the m/z 298.1797 ion. The inset to panel B shows the proposed structure and cleavage sites. * background ions. ** ammonium adduct of dimethylsulfone. *** $[M+H]^+$ ion of erucamide, a compound used in plastic manufacturing. *** ammonium adduct of erucamide.

3.4 Validation of the DART-MS results, synthesis of authentic reference standards, and GC-MS and LC-MS analysis for definitive identification and differentiation of the α -U10 and β -U10 isomers.

Several of the samples collected in this study contained sufficient visible residue to enable their extraction and analysis using GC-MS. For example, in the sample whose DART-MS spectra was shown in Figure 2D, observed the week of Sept 21st, 2020, a pale brown colored visible residue was present in the metal tray. This tray was subsequently extracted with methanol and subjected to GC-MS analysis (**Figure 10**). With the exception of diphenhydramine that was not observed

due to its thermal lability, the substances observed by GC-MS were consistent with those observed by DART-MS, including xylitol and heroin, and several other opioids present in raw opium including codeine, noscapine (identified by its thermal degradation product meconin) and papaverine [63,64], as well as synthesis or degradation products associated with heroin including acetylcodeine [65], 6-monoacetylmorphine and morphine (Figure 10A). In addition, a species eluting at 17.550 minutes, resulting in the Electron Ionization (EI)-MS spectrum shown in Figure 10B, was consistent with the reference spectrum for α -U10 in the SWGDrug monograph [53]. However, to determine if this corresponded to the α -U10 and/or β -U10 isomer, reference standards of both isomers were synthesized, and then characterized as their freebase forms via X-ray crystallography (Figure 1) Note that reference standards for both isomers are now available from Cayman Chemical, sold under the name 1-naphthoyl U-47700 and 2-naphthoyl U-47700, but were not available at the time of this work. GC-MS analysis of these standards using the same conditions as for the sample shown in Figure 10 resulted in a retention time for α -U10 of 17.161 minutes and 17.518 minutes for β -U10, consistent with the retention time of 17.550 minutes for the sample, thereby confirming its identity as β -U10. Additional confirmation was provided via LC-MS analysis, where the sample eluted at the same retention time as the β -U10 standard (7.66 min), whereas the α -U10 isomer eluted at 8.32 min. GC-MS and/or LC-MS analysis of multiple other DDP samples collected at different time points and in which visible residue was present, all provided results consistent with those observed by DART-MS, and confirmed that only β -U10 was present throughout this pilot study. Notably, the results reported here for identification and characterization of β -U10, and the absence of the α -U10 isomer, are entirely consistent with those reported in July 2021 by Collins *et. al.*, who described the identification of β -U10 in Australia through the analysis of samples seized by law enforcement agencies in December 2020 [66] i.e., several months after it was first observed in the study now reported here. The presence of β -U10 has since also been reported in Ohio, USA in May 2021 under the name 2-naphthoyl U-47700 [67].

Minimal information regarding the pharmacological properties of β -U10 is available in the literature. The United States Patent 4,215,144, where this compound was first described, states ‘This invention relates to N-(2-aminocycloaliphatic)- benzamides and naphthamides which have been found to be useful for relieving pain in animals’ [12], suggesting that during their studies the compound may have been found to exhibit some activity. U-47700 is a potent μ -opioid receptor

agonist, approximately 7.5 times more potent than morphine [68]. However, Hsu *et. al.*, who investigated a range of U- and A-series compounds interacting with human μ -opioid receptor 1 expressing cells [52], reported that α -U10 had no observable agonistic effects. Szmuszkovicz reported that conversion of benzamides to acetamides resulted in reduced μ -receptor activity whilst still retaining analgesic properties, leading to the observation that the modification may result in increased selectivity for the κ -receptor [68]. This was termed the “eastern methylene group’ effect. Subsequent studies of U-69593 [69] and U-50488 confirmed this κ -selectivity [70]. Finally, Halfpenny *et. al.* reported that several naphthalene derivatives of (+/-)-trans-N-methyl-N-[2-(1-pyrrolidinyl) cyclohexyl]benzo [b]thiophene-4-acetamide monohydrochloride (1,PD117302), which is an analogue of U50,488, have high κ -opioid receptor affinity, selectivity and potency [71]. This suggests that β -U10 may have selectivity and activity via the κ -opioid receptor. However, this remains to be determined.

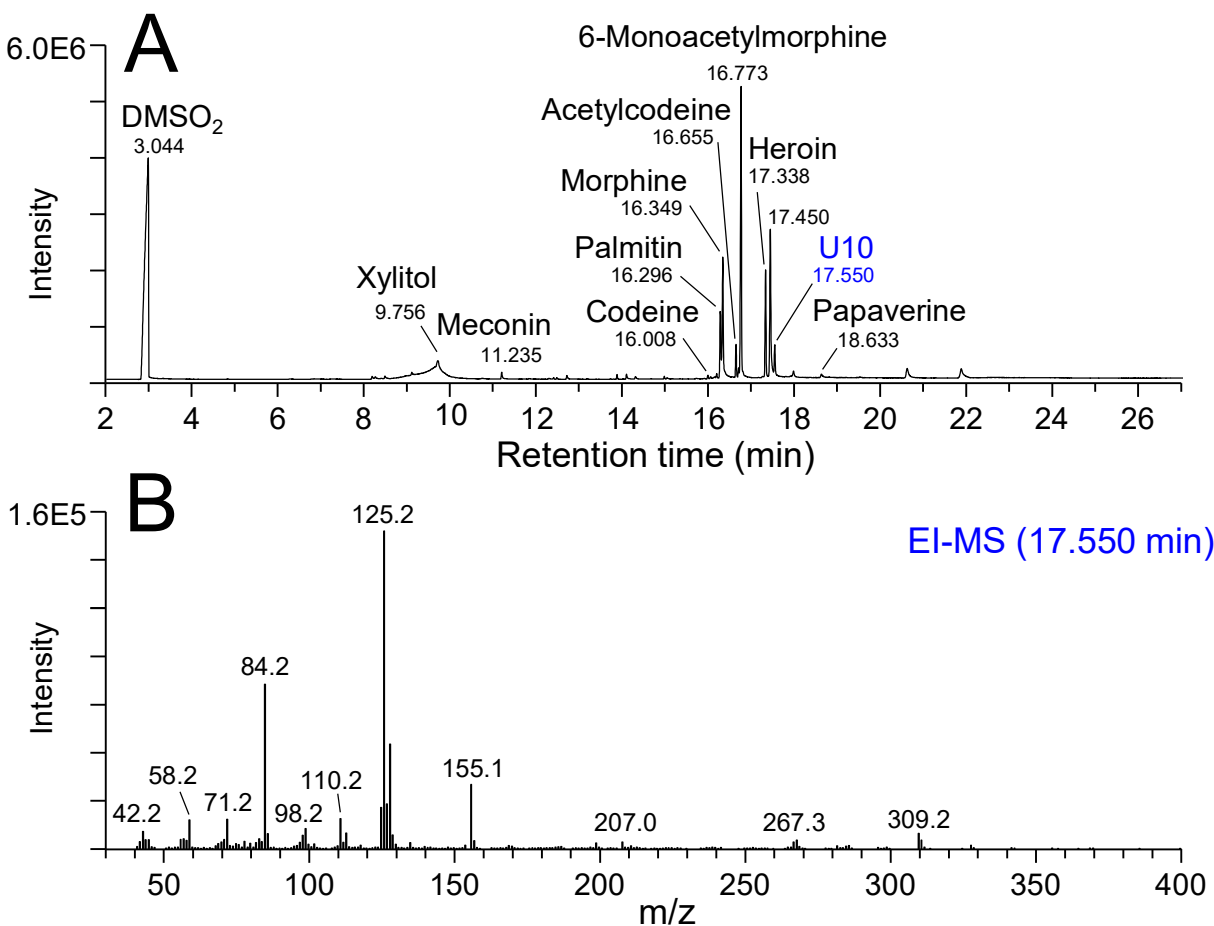


Figure 10. GC-MS analysis of a methanol extract from the content of the metal tray from Figure 2D. (A) GC trace (B) EI-MS spectra of the species eluting at 17.550 minutes, consistent with either α -U10 or β -U10.

3.5 213 nm photodissociation-MS/MS for differentiation of α -U10 and β -U10 isomers without need for chromatographic separation

Notably, the EI spectra obtained by GC-MS of the isomeric α -U10 and β -U10 reference standards, and the spectra obtained from the isomers using conventional HCD-MS/MS, were virtually indistinguishable from each other. For example, aside from a small difference in the ratio of product ions at m/z 126.13 and m/z 127.05 ions, corresponding to $C_8H_{16}N^+$ and $C_{10}H_7^+$ respectively, no unique product ions were observed for either species via HCD-MS/MS (**Figures 11A and 11B**, respectively). This suggests a necessity for chromatographic separation prior to MS analysis, not only for the characterization of novel drug substances, but also to provide definitive identifications when multiple isomeric species may be present. This requirement however, may limit throughput capacity for applications involving high throughput ‘street level’ drug monitoring, or where close to real time reporting is desired (particularly in field-based applications), due to the need to perform sample extraction prior to analysis and the relatively long timescales required for chromatographic analysis compared to using DART-MS. However, a range of alternate ion-activation/dissociation techniques have been developed in recent years, including UltraViolet-PhotoDissociation (UVPD), that provide access to fragmentation pathways not accessed using conventional collisional activated MS/MS methods and that enable ‘near complete’ structural characterization for a wide range of biomolecules including peptides, proteins, protein post translational modifications (PTM’s), and lipids, including for isomeric species, without need for chromatographic separations [72]. To date, however, the potential utility of UVPD-MS/MS for the isomeric structural elucidation or differentiation of pharmaceutical or illicit drug species has not been explored.

Here, 213 nm UVPD-MS/MS of α -U10 and β -U10 using a commercially available mass spectrometry platform resulted in formation of the same products as observed using conventional HCD-MS/MS along with a number of unique, albeit low relative abundance, product ions for both isomers (**Figure 12**). For example, the α -U10 isomer yielded a unique ion at m/z 169.0519

($C_{11}H_7NO^+$), corresponding to sequential cleavages of the cyclohexylamine and methylamine N-C bonds (Figure 12A), whereas the β -U10 isomer (Figure 12B) gave three unique ions, namely m/z 238.15 corresponding to the loss of CO and $N(CH_3)_2$, m/z 198.09 (loss of $C_7H_{15}N$) and m/z 169.06 (formation of $C_{12}H_9O^+$). These differences in fragmentation likely arise due to the 1- versus 2-naphthol substituted positions of the cyclohexylamide groups in the α -U10 and β -U10 isomers, and also that the N-methylamide bond in the α -U10 isomer adopted a *trans*- configuration while the β -U10 isomer adopted a *cis*- configuration (see Figure 1). These unique UVPD product ions, acquired using activation timescales and dissociation efficiencies similar to those used in conventional MS/MS strategies, clearly allow for the differentiation of these two isomers without the need for chromatographic separation. Therefore, UVPD has potential utility as a powerful new tool for the enhanced identification and analysis of novel illicit drug substances.

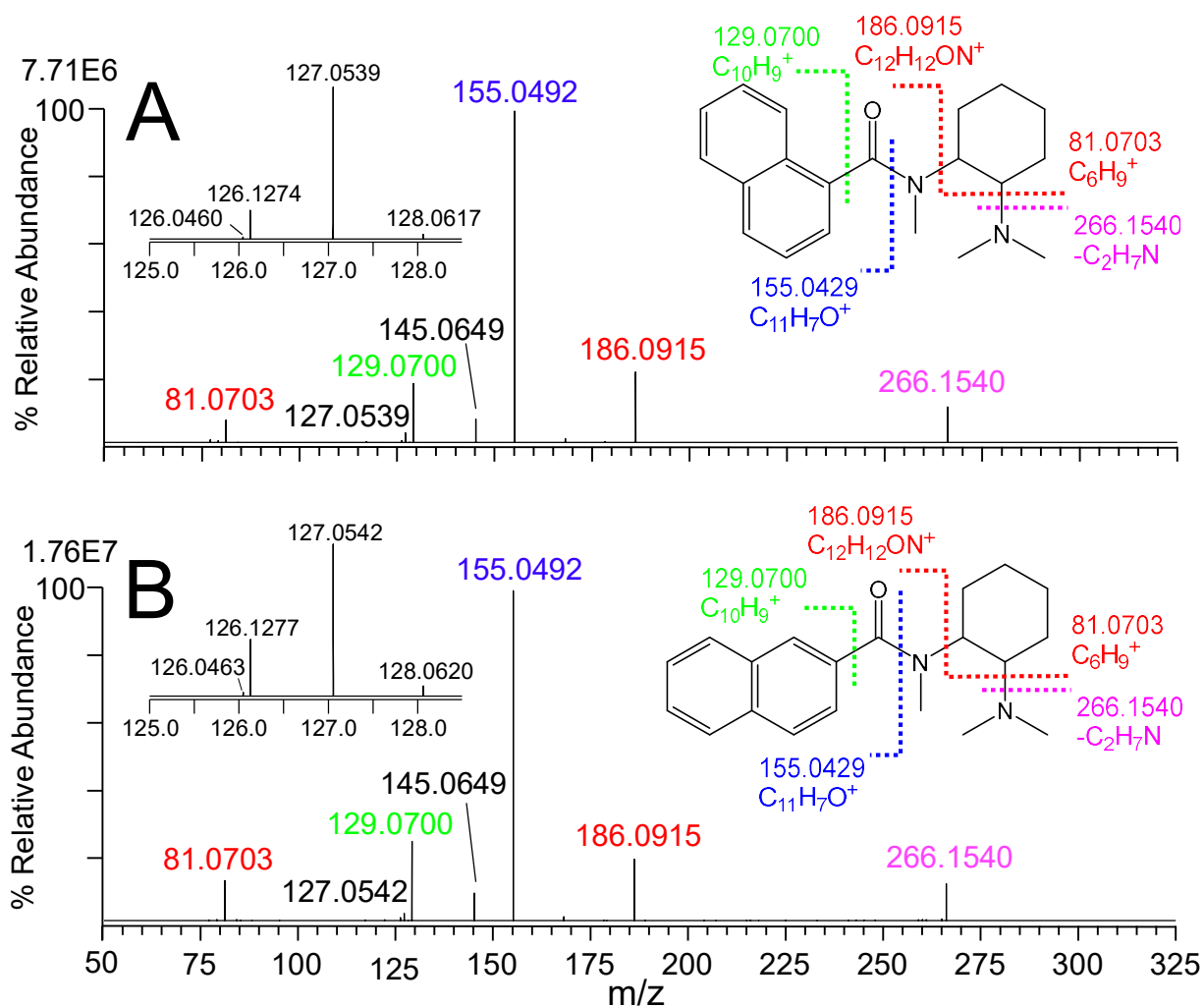


Figure 11. HCD-MS/MS spectra of A) α -U10 and B) β -U10 authentic reference standards. The insets show expanded regions of spectra from m/z 125-128, showing the differences in intensity ratios for two low abundance product ions. The inset structures in both panels show the proposed cleavage sites for each isomer.

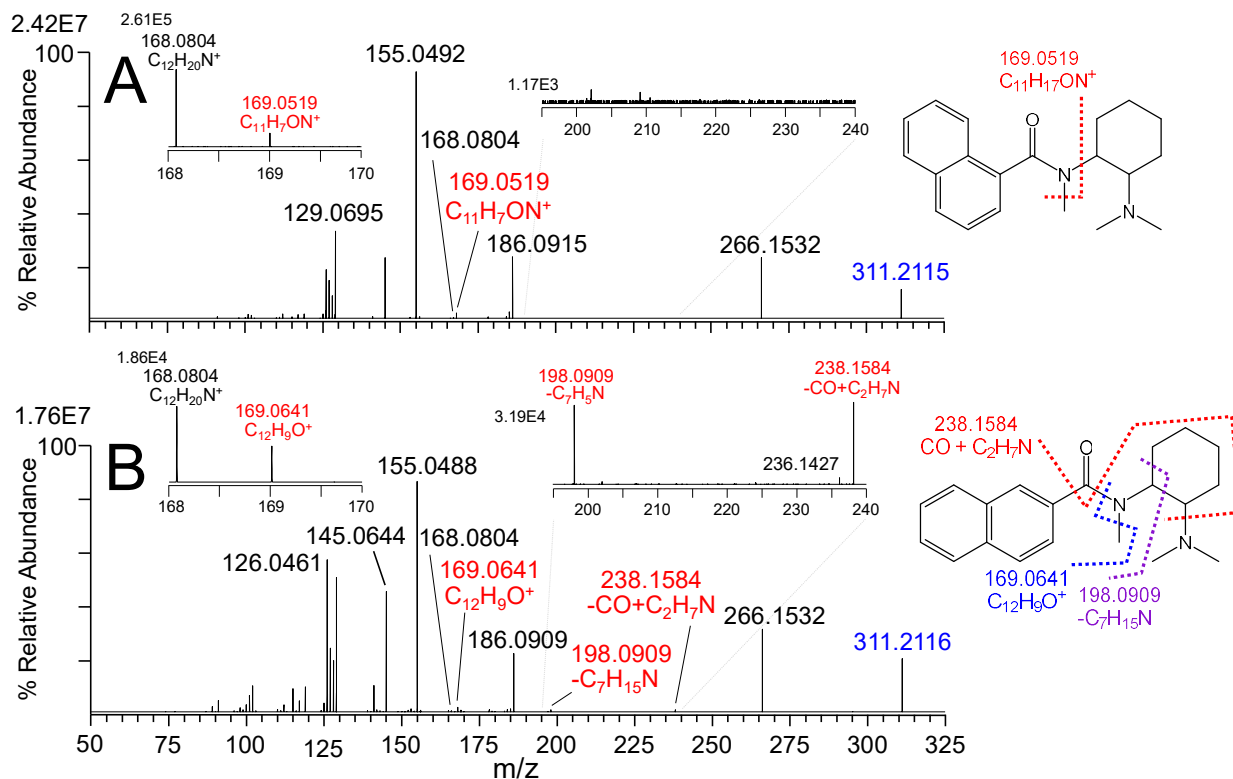


Figure 12. 213 nm UVPD-MS/MS of A) α -U10 and B) β -U10 synthetic reference standards. The insets in each panel show expanded regions of the spectra from m/z 168 - 170 and m/z 195 - 240. Unique product ions for each structure are highlighted in red. The inset structures show the proposed cleavage sites for the α -U10 and β -U10 isomers.

Conclusions

The identification and characterization of novel illicit drug substances predominately results from the analysis of seized samples using conventional analytical and forensic chemistry methods such as GC-MS, LC-MS and NMR. However, by the time this occurs it is likely that a drug is already in widespread use within the community. Here, trace-residue analysis of discarded drug paraphernalia using DART-MS and MS/MS, combined with advanced MS/MS methods such as UPVD, is demonstrated to be a powerful alternate method for (i) large-scale identification and monitoring of illicit drugs and complex poly-drug combinations at the point closest to where drug consumption occurs, (ii) monitoring longitudinal changes in the number and/or average signal intensity of a particular drug or poly-drug combination as proxy-indicators of changes in market conditions over time, and (iii) the identification and characterization of novel drug substances including novel synthetic opioids, that have not previously been reported.

Acknowledgements

We would like to acknowledge Dr Yukie O'Bryan and the Melbourne Trace Analysis for Chemical, Earth and Environmental Sciences (TrACEES) Platform at the University of Melbourne for acquiring the GC-MS data reported in this study. Funding for this study was provided from the Victoria State Government Department of Health.

References

1. Bade R, Tschärke BJ, O'Brien JW, Magsarjav S, Humphries M, Ghetia M, Thomas KV, Mueller JF, White JM, Gerber C. Impact of COVID-19 Controls on the Use of Illicit Drugs and Alcohol in Australia. *Environ Sci Technol Lett.* 2021;10:acs.estlett.1c00532.
2. Reinstadler V, Ausweger V, Grabher AL, Kreidl M, Huber S, Grandner J, Haslacher S, Singer K, Schlapp-Hackl M, Sorg M, Erber H, Oberacher H. Monitoring drug consumption in Innsbruck during coronavirus disease 2019 (COVID-19) lockdown by wastewater analysis. *Sci Total Environ.* 2021;757:144006.
3. Been F, Emke E, Matias J, Baz-Lomba JA, Boogaerts T, Castiglioni S, Campos-Mañas M, Celma A, Covaci A, de Voogt P, Hernández F, Kasprzyk-Hordern B, Laak TT, Reid M, Salgueiro-González N, Steenbeek R, van Nuijs ALN, Zuccato E, Bijlsma L. Changes in drug

- use in European cities during early COVID-19 lockdowns - A snapshot from wastewater analysis. *Environ Int.* 2021;153:106540.
4. Farhoudian A, Radfar SR, Mohaddes Ardabili H, Rafei P, Ebrahimi M, Khojasteh Zonoozi A, De Jong CAJ, Vahidi M, Yunesian M, Kouimtsidis C, Arunogiri S, Hansen H, Brady KT; ISAM Global Survey Consortium (ISAM-GSC), Potenza MN, Baldacchino AM, Ekhtiari H. A Global Survey on Changes in the Supply, Price, and Use of Illicit Drugs and Alcohol, and Related Complications During the 2020 COVID-19 Pandemic. *Front Psychiatry.* 2021;12:646206.
 5. Price O, Man N, Bruno R, Dietze P, Salom C, Lenton S, Grigg J, Gibbs D, Wilson T, Degenhardt L, Chan R, Thomas N, Peacock A. Changes in illicit drug use and markets with the COVID-19 pandemic and associated restrictions: findings from the Ecstasy and Related Drugs Reporting System, 2016-20. *Addiction.* 2022;117:182-194.
 6. Solimini R, Pichini S, Pacifici R, Busardò FP, Giorgetti R. Pharmacotoxicology of Non-fentanyl Derived New Synthetic Opioids. *Front Pharmacol.* 2018;9:654.
 7. Mather LE. Clinical pharmacokinetics of fentanyl and its newer derivatives. *Clin Pharmacokinet.* 1983;8:422-446.
 8. Armenian P, Vo KT, Barr-Walker J, Lynch KL. Fentanyl, fentanyl analogs and novel synthetic opioids: A comprehensive review. *Neuropharmacology.* 2018;134:121-132.
 9. Vardanyan RS, Hruby VJ. Fentanyl-related compounds and derivatives: current status and future prospects for pharmaceutical applications. *Future Med Chem.* 2014;6:385-412.
 10. Harper NJ, Veitch GB, Wibberley DG. 1-(3,4-Dichlorobenzamidomethyl)cyclohexyldimethylamine and related compounds as potential analgesics. *J Med Chem.* 1974;17:1188-1193.
 11. Harper NJ, Veitch GBA. Ethylene diamine derivatives. 1977, US. Patent US4049663A.
 12. Szmuszkovic J. Analgesic N-(2-(furylmethylamino and 2-thienylmethylamino)cycloaliphatic)benzamides. 1979, US. Patent US4153717A.
 13. Baumann MH, Tocco G, Papsun DM, Mohr AL, Fogarty MF, Krotulski AJ. U-47700 and Its Analogs: Non-Fentanyl Synthetic Opioids Impacting the Recreational Drug Market. *Brain Sci.* 2020;10:895.
 14. Coopman V, Blanckaert P, Van Parys G, Van Calenbergh S, Cordonnier J. A case of acute intoxication due to combined use of fentanyl and 3,4-dichloro-N-[2-(dimethylamino)cyclohexyl]-N-methylbenzamide (U-47700). *Forensic Sci Int.* 2016;266:68-72.
 15. Katselou M, Papoutsis I, Nikolaou P, Spiliopoulou C, Athanaselis S. AH-7921: the list of new psychoactive opioids is expanded. *Forensic Toxicol.* 2015;33:195-201.
 16. Mohr AL, Friscia M, Papsun D, Kacinko SL, Buzby D, Logan BK. Analysis of Novel Synthetic Opioids U-47700, U-50488 and Furanyl Fentanyl by LC-MS/MS in Postmortem Casework. *J Anal Toxicol.* 2016;40:709-717.
 17. Breindahl T, Kimergård A, Andreasen MF, Pedersen DS. Identification of a new psychoactive substance in seized material: the synthetic opioid N-phenyl-N-[1-(2-phenethyl)piperidin-4-yl]prop-2-enamide (Acrylfentanyl). *Drug Test Anal.* 2017;9:415-422.

18. Blanckaert P, Balcaen M, Vanhee C, Risseeuw M, Canfyn M, Desmedt B, Van Calenbergh S, Deconinck E. Analytical characterization of "etonitazepyne," a new pyrrolidinyll-containing 2-benzylbenzimidazole opioid sold online. *Drug Test Anal.* 2021;13:1627-1634.
19. Verougstraete N, Vandeputte MM, Lyphout C, Cannart A, Hulpia F, Van Calenbergh S, Verstraete AG, Stove C. First Report on Brorphine: The Next Opioid on the Deadly New Psychoactive Substance Horizon? *J Anal Toxicol.* 2021;44:937-946.
20. Néfau T, Charpentier E, Elyasmino N, Duplessy-Garson C, Levi Y, Karolak S. Drug analysis of residual content of used syringes: a new approach for improving knowledge of injected drugs and drug user practices. *Int J Drug Policy.* 2015;26:412-419.
21. Fiorentin TR, Logan BK. Analytical findings in used syringes from a syringe exchange program. *Int J Drug Policy.* 2020;81:102770.
22. Lefrançois E, Augsburg M, Esseiva P. Drug residues in used syringes in Switzerland: A comparative study. *Drug Test Anal.* 2018;10:874-879.
23. Lefrancois E, Belackova V, Silins E, Latimer J, Jauncey M, Shimmon R, Mozaner Bordin D, Augsburg M, Esseiva P, Roux C, Morelato M. Substances injected at the Sydney supervised injecting facility: A chemical analysis of used injecting equipment and comparison with self-reported drug type. *Drug Alcohol Depend.* 2020;209:107909.
24. Brunt TM, Lefrançois E, Gunnar T, Arponen A, Seyler T, Goudriaan AE, McAuley A, McKeown DA, Detrez V, Csorba J, Deimel D, Auwärter V, Kempf J, Karolak S, Nefau T. Substances detected in used syringes of injecting drug users across 7 cities in Europe in 2017 and 2018: The European Syringe Collection and Analysis Project Enterprise (ESCAPE). *Int J Drug Policy.* 2021;95:103130.
25. Gozdziński L, Aasen J, Larnder A, Ramsay M, Borden SA, Saatchi A, Gill CG, Wallace B, Hore DK. Portable gas chromatography-mass spectrometry in drug checking: Detection of carfentanil and etizolam in expected opioid samples. *Int J Drug Policy.* 2021;97:103409.
26. Dresen S, Ferreirós N, Gnann H, Zimmermann R, Weinmann W. Detection and identification of 700 drugs by multi-target screening with a 3200 Q TRAP LC-MS/MS system and library searching. *Anal Bioanal Chem.* 2010;396:2425-2434.
27. Di Rago M, Pantatan S, Hargreaves M, Wong K, Mantinieks D, Kotsos A, Glowacki L, Drummer OH, Gerostamoulos D. High Throughput Detection of 327 Drugs in Blood by LC-MS-MS with Automated Data Processing. *J Anal Toxicol.* 2021;45:154-183.
28. Morelato M, Beavis A, Kirkbride P, Roux C. Forensic applications of desorption electrospray ionisation mass spectrometry (DESI-MS). *Forensic Sci Int.* 2013;226:10-21.
29. Stojanovska N, Tahtouh M, Kelly T, Beavis A, Fu S. Qualitative analysis of seized cocaine samples using desorption electrospray ionization- mass spectrometry (DESI-MS). *Drug Test Anal.* 2015;7:393-400.
30. Vircks KE, Mulligan CC. Rapid screening of synthetic cathinones as trace residues and in authentic seizures using a portable mass spectrometer equipped with desorption electrospray ionization. *Rapid Commun Mass Spectrom.* 2012;26:2665-2672.
31. Vandergrift GW, Gill CG. Paper spray mass spectrometry: A new drug checking tool for harm reduction in the opioid overdose crisis. *J Mass Spectrom.* 2019;54:729-737.

32. Vandergrift GW, Hessels AJ, Palaty J, Krogh ET, Gill CG. Paper spray mass spectrometry for the direct, semi-quantitative measurement of fentanyl and norfentanyl in complex matrices. *Clin Biochem.* 2018;54:106-111.
33. Borden SA, Saatchi A, Vandergrift GW, Palaty J, Lysyshyn M, Gill CG. A new quantitative drug checking technology for harm reduction: Pilot study in Vancouver, Canada using paper spray mass spectrometry. *Drug Alcohol Rev.* 2022;41:410-418.
34. Jackson AU, Garcia-Reyes JF, Harper JD, Wiley JS, Molina-Díaz A, Ouyang Z, Cooks RG. Analysis of drugs of abuse in biofluids by low temperature plasma (LTP) ionization mass spectrometry. *Analyst.* 2010;135:927-933.
35. McCullough BJ, Patel K, Francis R, Cain P, Douce D, Whyatt K, Bajic S, Lumley N, Hopley C. Atmospheric Solids Analysis Probe Coupled to a Portable Mass Spectrometer for Rapid Identification of Bulk Drug Seizures. *J Am Soc Mass Spectrom.* 2020;31:386-393.
36. Grange AH, Sovocool GW. Detection of illicit drugs on surfaces using direct analysis in real time (DART) time-of-flight mass spectrometry. *Rapid Commun Mass Spectrom.* 2011;25:1271-1281.
37. Sisco ER, Verkouteren JR, Staymates JL, Lawrence JA. Rapid detection of fentanyl, fentanyl analogues, and opioids for on-site or laboratory based drug seizure screening using thermal desorption DART-MS and ion mobility spectrometry. *Forensic Chem.*, 2017;4:108-115.
38. Sisco E, Robinson EL, Burns A, Mead R. What's in the bag? Analysis of exterior drug packaging by TD-DART-MS to predict the contents. *Forensic Sci Int.* 2019;304:109939.
39. Brown, H, Oktem B, Windom A, Doroshenko V, Evans-Nguyen K. Direct Analysis in Real Time (DART) and a portable mass spectrometer for rapid identification of common and designer drugs on-site. *Forensic Chem.* 2016;1:66-73.
40. West H, Fitzgerald J, Hopkins K, Li E, Clark N, Tzanetis S, Greene SL, Reid GE. Early Warning System for Illicit Drug Use at Large Public Events: Trace Residue Analysis of Discarded Drug Packaging Samples. *J Am Soc Mass Spectrom.* 2021;32:2604-2614.
41. Nan Q, Hejian W, Ping X, Baohua S, Junbo Z, Hongxiao D, Huosheng Q, Fenyun S, Yan S. Investigation of Fragmentation Pathways of Fentanyl Analogues and Novel Synthetic Opioids by Electron Ionization High-Resolution Mass Spectrometry and Electrospray Ionization High-Resolution Tandem Mass Spectrometry. *J Am Soc Mass Spectrom.* 2020;31:277-291.
42. Moorthy AS, Kearsley AJ, Mallard WG, Wallace WE. Mass spectral similarity mapping applied to fentanyl analogs. *Forensic Chem.* 2020;19:10.1016/j.forc.2020.100237.
43. Davidson JT, Piacentino EL, Sasiene ZJ, Abiedalla Y, DeRuiterd J, Clark CR, Berden G, Oomens J, Ryzhov, V, Jackson GP. Identification of novel fragmentation pathways and fragment ion structures in the tandem mass spectra of protonated synthetic cathinones. *Forensic Chemistry*, 2020;19:100245.
44. Sekuła K, Wrzesień-Tokarczyk W, Stanaszek R, Byrska B, Zuba D. Analysis of Fragmentation Pathways of Fentanyl Derivatives by Electrospray Ionisation High-Resolution Mass Spectrometry. *Rapid Commun Mass Spectrom.* 2022;13:e9254.
45. <https://www.npsdiscovery.org/reports/monographs/>.
46. Adusumilli R, Mallick P. Data Conversion with ProteoWizard msConvert. *Methods Mol Biol.* 2017;1550:339-368.

47. Bald T, Barth J, Niehues A, Specht M, Hippler M, Fufezan C. pymzML--Python module for high-throughput bioinformatics on mass spectrometry data. *Bioinformatics*. 2012;28:1052-1053.
48. Sheldrick GM. Crystal structure refinement with SHELXL. *Acta Crystallographica Section C*. 2015;71:3-8.
49. Macrae CF, Bruno IJ, Chisholm JA, Edgington PR, McCabe P, Pidcock E, Rodriguez-Monge L, Taylor R, van de Streek J, Wood PA. Mercury CSD 2.0– new features for the visualization and investigation of crystal structures. *J. Appl. Cryst.* 2008;41:466-470.
50. Farrugia LJ. WinGX suite for small-molecule single-crystal crystallography. *J Appl Cryst.* 1999;32:837-838.
51. Nielsen S, McAuley A. Etizolam: A rapid review on pharmacology, non-medical use and harms. *Drug Alcohol Rev.* 2020;39:330-336.
52. Hsu T, Mallareddy JR, Yoshida K, Bustamante V, Lee T, Krstenansky JL, Zambon AC. Synthesis and pharmacological characterization of ethylenediamine synthetic opioids in human μ -opiate receptor 1 (OPRM1) expressing cells. *Pharmacol Res Perspect.* 2019;7:e00511.
53. <https://swgdrug.org/Monographs/U10.pdf>
54. Kronstrand R, Thelander G, Lindstedt D, Roman M, Kugelberg FC. Fatal intoxications associated with the designer opioid AH-7921. *J Anal Toxicol.* 2014;38:599-604.
55. Fels H, Lottner-Nau S, Sax T, Roider G, Graw M, Auwärter V, Musshoff F. Postmortem concentrations of the synthetic opioid U-47700 in 26 fatalities associated with the drug. *Forensic Sci Int.* 2019;301:e20-e28.
56. Kraemer M, Boehmer A, Madea B, Maas A. Death cases involving certain new psychoactive substances: A review of the literature. *Forensic Sci Int.* 2019;298:186-267.
57. Elliott, S. P., Brandt, S. D., and Smith, C. The first reported fatality associated with the synthetic opioid 3,4-dichloro-N-[2-(dimethyl amino)cyclohexyl]-N-methylbenzamide (U-47700) and implications for forensic analysis. *Drug Test Anal.* 2016;8:875–879.
58. Coopman, V., Blanckaert, P., Van Parys, G., Van Calenbergh, S., and Cordonnier, J. A case of acute intoxication due to combined use of fentanyl and 3,4-dichloro-N-[2-(dimethylamino)cyclohexyl]-N-methylbenzamide (U-47700). *Forensic Sci. Int.* 2016;266:68-72.
59. Sharma KK, Hales TG, Rao VJ, NicDaeid N, McKenzie C. The search for the "next" euphoric non-fentanil novel synthetic opioids on the illicit drugs market: current status and horizon scanning. *Forensic Toxicol.* 2019;37:1-16.
60. Fleming SW, Cooley JC, Johnson L, Frazee CC, Domanski K, Kleinschmidt K, Garg U. Analysis of U-47700, a Novel Synthetic Opioid, in Human Urine by LC-MS-MS and LC-QToF. *J Anal Toxicol.* 2017;41:173-180.
61. Poplawska M, Bednarek E, Naumczuk B, Kozerski L, Błażewicz A. Identification and structure characterization of five synthetic opioids: 3,4-methylenedioxy-U-47700, o-methyl-acetylfentanyl, 2-thiophenefentanyl, benzoylfentanyl and benzoylbenzylfentanyl. *Forensic Toxicol.*, 2021;39:45-58
62. <https://www.swgdrug.org/Monographs/A10%20HCl.pdf>

63. Paterson S, Cordero R. Comparison of the various opiate alkaloid contaminants and their metabolites found in illicit heroin with 6-monoacetyl morphine as indicators of heroin ingestion. *J Anal Toxicol.* 2006;30:267-273.
 64. Bogusz MJ, Maier RD, Erkens M, Kohls U. Detection of non-prescription heroin markers in urine with liquid chromatography-atmospheric pressure chemical ionization mass spectrometry. *J Anal Toxicol.* 2001;25:431-438.
 65. O'Neal CL, Poklis A, Lichtman AH. Acetylcodeine, an impurity of illicitly manufactured heroin, elicits convulsions, antinociception, and locomotor stimulation in mice. *Drug Alcohol Depend.* 2001;65:37-43.
 66. Collins M, Brown D, Davies S, Chan B, Trotter B, Moawad M, Blakey K, Collins-Brown L. Case study: Identification and characterization of N-[2-(dimethylamino)cyclohexyl]-N-methylnaphthalene-2-carboxamide, a regioisomer of the synthetic opioid U10. *Drug Test Anal.* 2022;14:188-195.
 67. https://www.nflis.deadiversion.usdoj.gov/nflisdata/docs/NFLIS_Synth-Opioids_2-naphthyl_U47700.pdf.
 68. Szmuszkowicz J, Von Voigtlander PF. Benzeneacetamide amines: structurally novel non- μ opioids. *J Med Chem.* 1982;25:1125-1116.
 69. La Regina A, Petrillo P, Sbacchi M, Tavani A. Interaction of U-69,593 with μ -, α - and κ -opioid binding sites and its analgesic and intestinal effects in rats. *Life Sci.* 1988;42:293-301.
 70. Vonvoigtlander PF, Lahti RA, Ludens JH. U-50,488: a selective and structurally novel non- μ (κ) opioid agonist. *J Pharmacol Exp Ther.* 1983;224:7-12.
 71. Halfpenny PR, Horwell DC, Hughes J, Humblet C, Hunter JC, Neuhaus D, Rees DC. Highly selective κ opioid analgesics. 4. Synthesis of some conformationally restricted naphthalene derivatives with high receptor affinity and selectivity. *J Med Chem.* 1991;34, 190-194.
 72. Brodbelt JS, Morrison LJ, Santos I. Ultraviolet Photodissociation Mass Spectrometry for Analysis of Biological Molecules. *Chem Rev.* 2020;120:3328-3380.
-